Available online at www.sciencedirect.com
ScienceDirect
Journal of Nuclear Materials 373 (2008) 82–89
journal of nuclear materials
www.elsevier.com/locate/jnucmat

Creep constitutive equation of dual phase 9Cr-ODS steel

Hideo Sakasegawa [a,*], Shigeharu Ukai [a,1], Manabu Tamura [b], Satoshi Ohtsuka [a], Hiroyasu Tanigawa [c], Hiroyuki Ogiwara [c], Akira Kohyama [d], Masayuki Fujiwara [a]

[a] Advanced Nuclear System Research and Development Directorate, Japan Atomic Energy Agency, 4002 Narita-cho, Oarai-machi, Higahi-Ibaraki-gun, Ibaraki-ken 311-1393, Japan
[b] Department of Materials Science and Engineering, National Defense Academy, 1-10-20 Hashirimizu, Yokosuka-shi, Kanagawa-ken 239-8686, Japan
[c] Naka Fusion Institute, Japan Atomic Energy Agency, 2-4 Shirakata, Tokai-mura, Ibaraki-ken 319-1195, Japan
[d] Institute of Advanced Energy, Kyoto University, Gokasho, Uji-shi, Kyoto-fu 611-0011, Japan

Received 7 July 2006; accepted 8 May 2007

Abstract

9Cr-ODS (oxide dispersion strengthened) steels developed by JAEA (Japan Atomic Energy Agency) have superior creep properties compared with conventional heat resistant steels. The ODS steels can enormously contribute to practical applications of fast breeder reactors and more attractive fusion reactors. Key issues are developments of material processing procedures for mass production and creep life prediction methods in present R&D. In this study, formulation of creep constitutive equation was performed against the backdrop. The 9Cr-ODS steel displaying an excellent creep property is a dual phase steel. The ODS steel is strengthened by the δ ferrite which has a finer dispersion of oxide particles and shows a higher hardness than the α' martensite. The δ ferrite functions as a reinforcement in the dual phase 9Cr-ODS steel. Its creep behavior is very unique and cannot be interpreted by conventional theories of heat resistant steels. Alternative qualitative model of creep mechanism was formulated at the start of this study using the results of microstructural observations. Based on the alternative creep mechanism model, a novel creep constitutive equation was formulated using the exponential type creep equation extended by a law of mixture.

PACS: 62.20.Hg; 61.72.Ff; 61.72.Hh

1. Introduction

9Cr-ODS steels developed by JAEA have superior creep properties compared with conventional heat resistant steels. The creep rupture strength (1000 h at 973 K) is about 10 times greater than conventional heat resistant steels [1–5]. The steel can enormously contribute to practical applications of fast reactors and more attractive fusion reactors [6–9]. The superior creep property results from a high number density of small Y–Ti–O and/or Ti–O oxide particles dispersed in the matrix. These particles improve the creep property by pinning and piling up moving dislocations at elevated temperatures. In most of researches on ODS steels, material designs and material processing procedures were accordingly focused to finely disperse oxide particles. Few studies on the creep mechanism are reported [1,6,9] using the power law type equation. Stress exponent values can explain simple creep mechanisms. However, detailed creep mechanisms cannot be interpreted. The power law type equation is an empirical rule and has few physical meanings. Our researches reveal that the 9Cr-ODS steel has an excellent creep property is a dual phase steel which is consist of δ ferrite and α' martensite. [1–5]. The ODS steel has very unique creep behaviors, which were not observed in conventional heat resistant steels. Analyses using the power law type equation cannot consequently

* Corresponding author. Tel.: +81 29 267 4141; fax: +81 29 267 7173.
E-mail address: hideo.sakasegawa@cea.fr (H. Sakasegawa).
[1] Present address: Department of Materials Science and Engineering, Hokkaido University, Kita 8 Nishi 5, Kita-ku, Sapporo-shi, Hokkaido 060-0808, Japan.

0022-3115/$ - see front matter © 2007 Elsevier B.V. All rights reserved.
doi:10.1016/j.jnucmat.2007.05.031

Nomenclature

List of symbols

α'	martensite
δ	delta ferrite
σ	applied stress
σ_y	yield stress
$\sigma_{0.2}$	0.2% proof stress
$\sigma_{y,i}$	yield stress in i phase ($i = \alpha'$, δ)
$\sigma_{0.2,}$	0.2% proof stress in i phase ($i = \alpha'$, δ)
f_δ	volume fraction of delta ferrite
HV_i	Vickers hardness in i phase ($i = \alpha'$, δ)
R	gas constant
T	temperature in K
$\dot{\varepsilon}$	macroscopic creep strain rate
$\dot{\varepsilon}_i$	creep strain rate in i phase ($i = \alpha'$, δ)
$\dot{\varepsilon}_{disl.,\alpha'}$	dislocation gliding creep strain rate in α'
$\dot{\varepsilon}_{g.b.s.,\alpha'}$	grain boundary sliding creep strain rate in α'
$\dot{\varepsilon}_0$	constant
$\dot{\varepsilon}_{0,i}$	constant in i phase ($i = \alpha'$, δ)
t_{r0}	constant
$t_{r0,i}$	constant in i phase ($i = \alpha'$, δ)
Q	activation energy in the absence of applied stress
Q_i	activation energy in the absence of applied stress in i phase ($i = \alpha'$, δ)
Q_d	activation energy for self-diffusion
$Q_{d,i}$	activation energy for self-diffusion in i phase ($i = \alpha'$, δ)
Q_{int}	elastic interaction energy between movable dislocations and obstacle dislocations
$Q_{int,i}$	elastic interaction energy between movable dislocations and obstacle dislocations in i phase ($i = \alpha'$, δ)
V	activation volume
V_i	activation volume in i phase ($i = \alpha'$, δ)
μ	shear modulus
μ_i	shear modulus in i phase ($i = \alpha'$, δ)
p	characteristic parameter for obstacle dislocation
p_i	characteristic parameter for obstacle dislocation in i phase ($i = \alpha'$, δ)
d	spacing of obstacle dislocations
d_i	spacing of obstacle dislocations in i phase ($i = \alpha'$, δ)
b	length of Burger's vector
ν	Poisson's ratio
r_0	length between the nearest neighbor atoms
d/p	EOS: equivalent obstacle spacing
d_i/p_i	EOS: equivalent obstacle spacing in i phase ($i = \alpha'$, δ)

give available information to completely study the creep mechanism. Alternative creep mechanism should be studied using results of microstructural observations, and novel analysis method should be established for the dual phase 9Cr-ODS steel. In addition, R&D on fast reactor fuel cladding tubes is moving to performance demonstrations from material and fuel pin system developments. Key issues are developments of material processing procedures for mass production and creep life prediction methods in the present step.

In this study, formulation of a creep constitutive equation based on detailed microstructural observations was performed to develop reliable life prediction methods against the backdrop.

2. Experimental procedure

The chemical composition of the dual phase 9Cr-ODS steel, as shown in Table 1, was prepared by MA (mechanical alloying) of argon-gas-atomized pre-alloyed metal powder along with Y_2O_3 powder in a high-energy attritor in an argon atmosphere for 48 h at 220 rpm (revolutions per minute). MA powder was then degassed at 673 K in vacuum (0.1 Pa), after which it was canned in mild steel and hot extruded at 1423 K into bar. This bar was drilled and machined to form a cladding tube with real dimension of 8.5 mm outer diameter and 0.5 mm thickness [1]. Normalizing and tempering conditions are 1323 K × 1 h/AC (air cooling) and 1073 K × 1 h/AC, respectively. Creep rupture tests were conducted at 923 and 973 K in air. The dimensions of the specimen used are shown in Fig. 1. This specimen was made from the cladding tube. These creep property data are for specimens taken in the extrusion direction. Vickers hardness tests were performed to investigate hardnesses (yield strengths) in each of matrixes. Microstructural observations were performed using SEM (scanning electron microscope), EPMA (electron probe micro analysis), and TEM (transmission electron

Table 1
The chemical composition of the dual phase 9Cr-ODS steel

	C	Cr	W	Ti	Y	O	Fe	Y_2O_3
(wt%)	0.14	8.9	2.0	0.20	0.27	0.16	Bal.	0.34

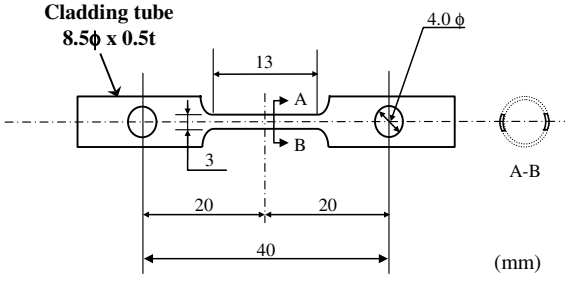

Fig. 1. The specimen dimensions.

microscope) to study the creep deformation and rupture mechanisms.

3. Result and discussion

3.1. Reinforcing effect of δ ferrite on creep property of dual phase 9Cr-ODS steel

Fig. 2 shows the typical reinforcing effect of the δ ferrite on the creep property of the dual phase 9Cr-ODS steel. The creep property is considerably improved by the δ ferrite. Matrix phases in 9Cr- ODS steels can be easily changed by controlling the oxygen content [3,4]. The dual phase 9Cr-ODS steel is produced at the total oxygen content of ≈0.13 wt%. δ ferrite is considered to be an unfavorable phase in conventional heat resistant steels, but the phase has an extremely important role in improving the creep property of the dual phase 9Cr-ODS steel.

Fig. 3(a) shows microstructures of the dual phase 9Cr-ODS steel. These structures were very different from those of conventional heat resistant steels. For example, prior austenite grain sizes in the α′ martensite of ODS steels were about 5 μm. These sizes are very small compared with the conventional steels. In addition, our recent investigation using EBSP (electron back scattering pattern) measurement shows that there are unique orientations of subgrain boundaries in the α′ martensite. The δ ferrite shape can be easily seen in the result of EPMA mapping of Cr (a ferrite forming element). This phase was elongated parallel to the extrusion direction. It was 50–100 μm long and about 10 μm across. The volume fraction was about 0.25.

TEM observations revealed that the δ ferrite has a finer dispersion of oxide particles than the α′ martensite, as shown in Fig. 3(a). The δ ferrite shows a higher hardness, in agreement with the TEM observation results. It probably functions as a reinforcement in the dual phase 9Cr-ODS steel. The microstructures of the dual phase 9Cr-ODS steel were illustrated in Fig. 3(b). These structures resemble structures of a fiber reinforced composite material when considering that the δ ferrite functions as a reinforcement. This consideration is discussed in the following.

Fig. 4(a) shows the result of Vickers hardness test. The test using the smaller indent sizes proves the presence of two different areas, hard and soft areas, while the test using the larger indent sizes approaches a common value. These results are consistent with that the dual phase 9Cr-ODS steel is consist of two matrixes, δ ferrite and α′ martensite, as shown in Fig. 3. Using these values, the correlation between volume fraction of the δ ferrite and σ_y are shown in Fig. 4(b). These data were summarized applying the law of mixture for the continuous fiber composite:

$$\begin{cases} \sigma_y = (1-f_\delta)\sigma_{y,\alpha'} + f_\delta \sigma_{y,\delta}, \\ \qquad\qquad\qquad\qquad (i = \alpha', \delta). \\ \sigma_{y,i} \approx \sigma_{0.2,i} \approx 3\mathrm{HV}_i, \end{cases} \tag{1}$$

An experimental result obtained by a tensile test is also plotted in the figure. From the result, f_δ is estimated to be about 0.25. This value is quite similar to the value obtained by the EPMA mapping.

These results support that the dual phase 9Cr-ODS steel can be characterized as a continuous fiber reinforced composite and concluded that the effect of composite should be considered to clarify the creep mechanism of the dual phase 9Cr-ODS steel. Reasons why the dual phase 9Cr-ODS steel can be characterized as a continuous fiber reinforced composite are probably as follows:

1. The interface strength between δ ferrite and α′ martensite is probably enough to transfer stress, because the dual phase 9Cr-ODS steel is not an artificial composite.
2. The difference in yield strength between δ and α′ is not large. The yield strength ratio is estimated to be about 1.2 [10].

It should be noted that these results can be applied to the condition that the applied stress direction is parallel to the extrusion direction.

3.2. Qualitative model of creep mechanism

The typical creep deformation curve of the dual phase 9Cr-ODS steel is shown in Fig. 5. Acceleration creep was not observed. The steel had a very low strain and ruptured in a brittle fracture mode. Such creep behaviors are not be observed in conventional heat resistant steels. Alternative qualitative model of creep mechanism should be formulated using the results of microstructural observations.

Fig. 6(a) shows the grain boundary sliding in the α′ martensite. As long as the strain induced by the grain boundary sliding mechanism in the α′ martensite is relaxed by the intragranular dislocation climb and glide mechanism, the ODS steel can go on the creep deformation. In other words, the grain boundary sliding mechanism cooperates with the intragranular dislocation climb and glide creep mechanism during the creep deformation, as shown in Fig. 7(a). Creep cavities were formed on PPB (prior particle boundaries) during the creep deformation. They were aligned along the extrusion direction and observed as 'stringer' in the commercial ODS steel, MA957 [6]. Interfacial

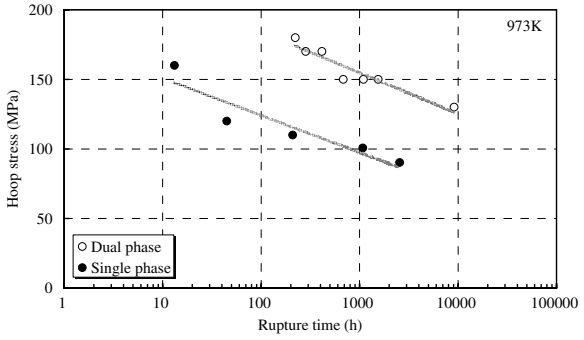

Fig. 2. The improved creep property by the δ ferrite.

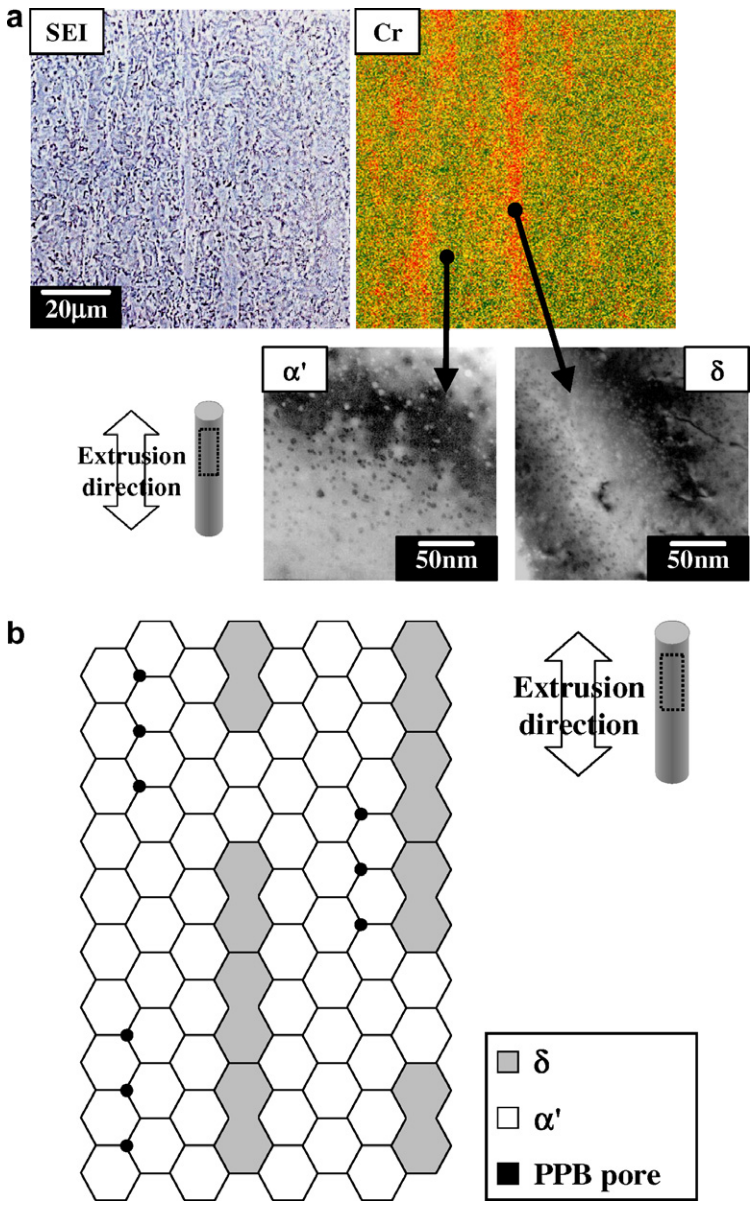

Fig. 3. Microstructures of the dual phase 9Cr-ODS steel: (a) Microstructures and (b) the schematic model.

peelings between PPB formed the creep cavities. They did not affect the creep deformation behavior consequently. The interfacial peelings were assisted by the PPB pores, where coarse titanium oxides of ≈5 μm were found in 9Cr ODS steels [11,12].

In Fig. 5, the creep strain rate gradually decreased with increasing strain. It means that work hardening occurred during the creep deformation. In other words, the intragranular dislocation climb and glide mechanism became difficult to function, because very stable oxide particles pinned and piled up moving dislocations at elevated temperatures. When the intragranular dislocation climb and glide mechanism cannot finely relax the strain induced by the grain boundary sliding mechanism, a creep crack is formed on a triple junction of grain boundaries in the α' martensite and immediately propagates, as shown in Figs. 7(b) and (c). These PPB creep cavities were linked up by the creep crack propagation perpendicular to the extrusion direction, as shown Fig. 7(b). These creep deformation and rupture mechanisms can interpret the low strain and the brittle fracture mode.

3.3. Quantitative model of creep mechanism

3.3.1. Exponential type creep constitutive equation

Creep properties have generally been studied using the power law type equation in most of researches on high temperature materials. It is very convenient to use the equation for summarizing and discussing creep properties. Fig. 8 shows the correlation between applied stress and minimum creep strain rate when using the equation. It is well known that values of stress exponent, n, explain creep

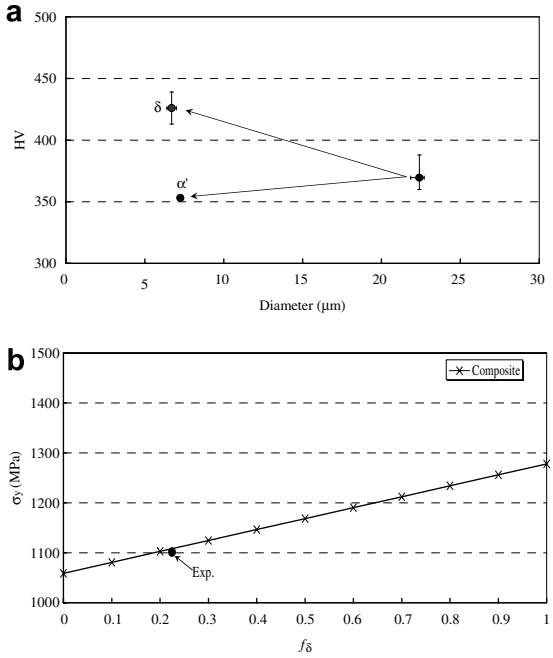

Fig. 4. The reinforcing effect of the δ ferrite summarize by using the law of mixture: (a) Vicker's hardness and (b) yield stress (≈0.2% proof stresses).

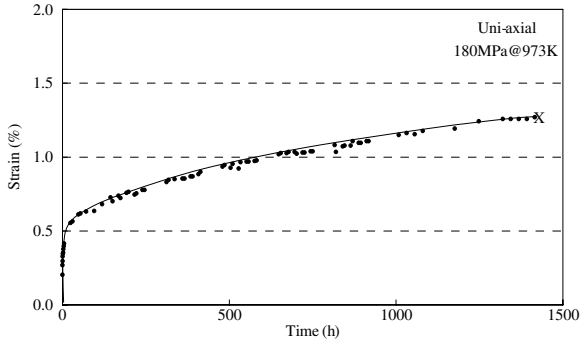

Fig. 5. The typical creep deformation curve of the dual phase 9Cr-ODS steel.

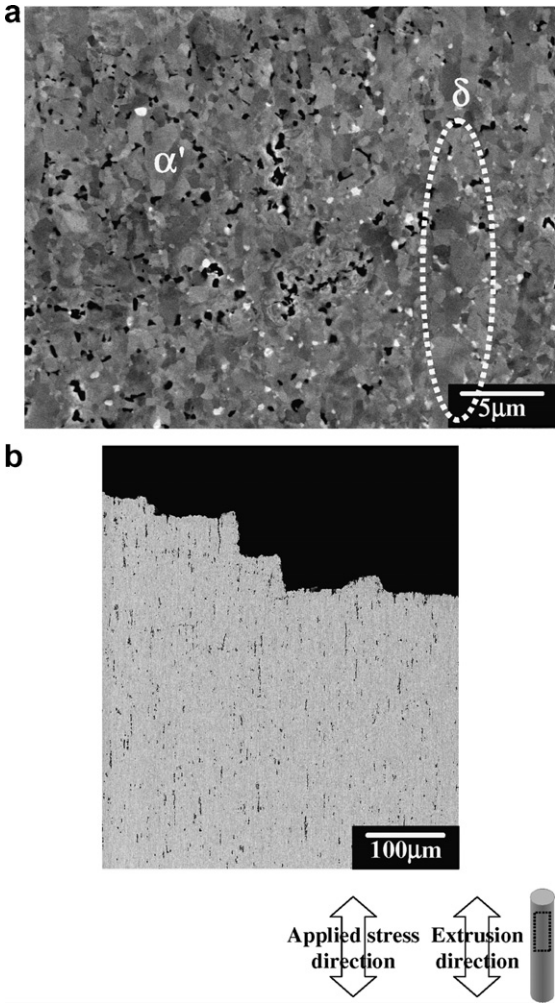

Fig. 6. Creep mechanisms: (a) the grain boundary sliding mechanism in the α' martensite and (b) the creep rupture.

mechanisms. However, the obtained values were much higher than those of dislocation climb and glide creep mechanism of 3–5. The values cannot give available information to completely clarify the creep mechanism of the dual phase 9Cr-ODS steel. Detailed creep mechanisms cannot be interpreted from the result, because the power law type equation is an empirical rule and has few physical meanings. In particular, the 9Cr-ODS steel has an excellent creep property is a dual phase steel. The δ ferrite functions as a reinforcement for improving the creep property. Its creep behavior is very unique and cannot be interpreted by conventional theories of heat resistant steels. A novel equation should be formulated based on a physical creep model.

In recent studies on creep mechanisms, the exponential type equation has been applied to many heat resistant steels by Tamura et al. [13–16]. It is shown that this application is available for summarizing and discussing creep properties. The physical creep model of the exponential type equation is based on thermally-activated process considering a decrease in free energy due to the load drop [13]. The creep rupture time, t_r, is expressed as

$$t_r = t_{r0} \exp\left(\frac{Q - \sigma V}{RT}\right), \tag{2}$$

where σ, T, R, Q, V, and t_{r0} are the applied stress, the testing temperature in K, the gas constant the activation energy in the absence of the applied stress, the activation volume, and the constant, respectively. Advantages of the exponential type equation application are as follows:

1. Long-term creep rupture strengths can easily be extrapolated, because the applied stress is correlated linearly with the logarithm of creep rupture time.
2. The material constants, Q, V, t_{r0}, which are calculated from the exponential type equation, can precisely interpret creep behaviors.

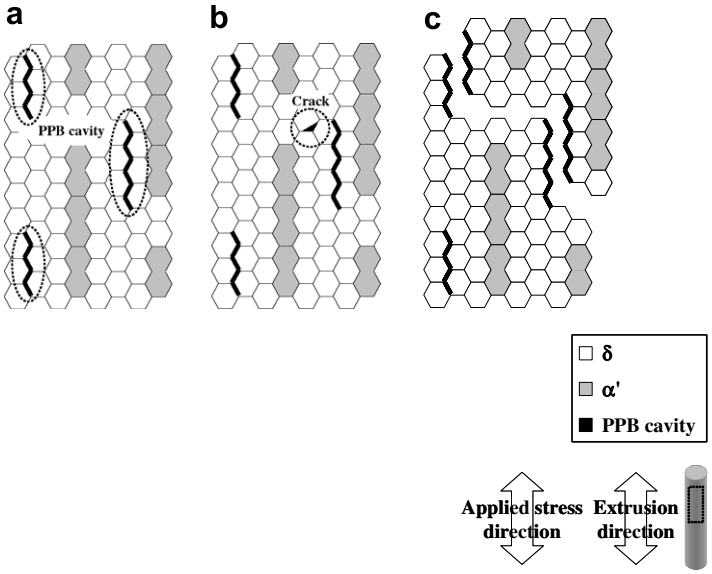

Fig. 7. Schematic models of creep mechanisms: (a) deformation, (b) crack initiation and (c) rupture.

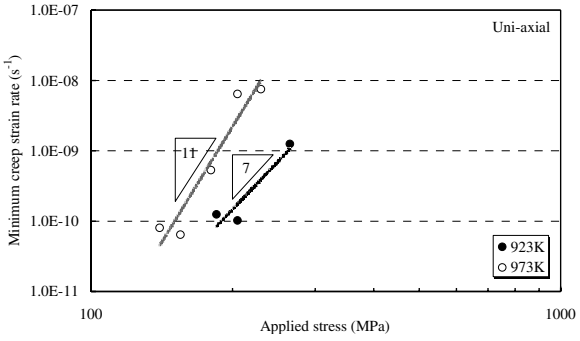

Fig. 8. Correlations between applied stress and minimum creep strain rate summarized by the power law type equation.

The intragranular dislocation climb and glide creep mechanism cooperates with the grain boundary sliding mechanism during the creep deformation. The creep strain rate can be represented by the rate of the intragranular dislocation climb and glide creep mechanism. Accordingly, the exponential type equation is applied in this study. It indicates the creep strain rate by the following equation:

$$\dot{\varepsilon} = \dot{\varepsilon}_0 \exp\left(-\frac{Q-\sigma V}{RT}\right), \tag{3}$$

where $\dot{\varepsilon}$ is the creep strain rate. $\dot{\varepsilon}_0$ is the constant. Q, V and the other constants can be calculated from the creep rupture test results which are summarized by the exponential type equation [14]. d/p(EOS: equivalent obstacle spacing) can be calculated using the equations as follows:

$$\begin{cases} Q = Q_{\mathrm{d}} + Q_{\mathrm{int}}\left(1 - \frac{\mathrm{d}\ln\mu}{\mathrm{d}\ln T}\right), \\ \frac{d}{p} = \frac{\mu b}{\pi(1-\nu)} \ln\left(\frac{d}{2r_0}\right)\frac{V}{Q_{\mathrm{int}}}. \end{cases} \tag{4}$$

EOS denotes the effective obstacle spacing influencing the moving dislocation. Q_{d} is the activation energy for self-diffusion. Q_{int} is the elastic interaction energy between the moving dislocation and the obstacle dislocation, μ is the shear modulus, p is the characteristic parameter for obstacle dislocation, d is the spacing of obstacle dislocations, b is the length of Burger's vector, ν is the Poisson's ratio, and r_0 is the length between the nearest neighbor atoms. It is reported that the value of EOS ($p \approx 1$) roughly coincide with inter particle spacing and/or subgrain size observed by TEM in many conventional heat resistant steels [13–16].

However, this formula cannot be directly applied to the dual phase 9Cr ODS steel. It should be modified and extended by the law of mixture, as discussed in Section 3.1.

3.3.2. Exponential type creep constitutive equation extended by law of mixture

Creep constitutive equation of the dual phase 9Cr-ODS should be formulated applying a law of mixture. Creep behaviors of composites have been studied by Wakashima et al. [17,18]. They used the power law type equation to their analyses which cannot be applied to the ODS steel.

Using the law of mixture of continuous fiber composite, the applied stress σ can be expressed with two stresses $\sigma_{\alpha'}$ and σ_δ [18]:

$$\begin{cases} \sigma = (1-f_\delta)\sigma_{\alpha'} + f_\delta\sigma_\delta, \\ \sigma_{\alpha'} = \frac{1-f_\delta\mathscr{B}}{1-f_\delta}\sigma - f_\delta\mathscr{A}(\varepsilon_{\alpha'} - \varepsilon_\delta), \\ \sigma_\delta = \mathscr{B}\sigma + (1-f_\delta)\mathscr{A}(\varepsilon_{\alpha'} - \varepsilon_\delta), \end{cases} \tag{5}$$

and

$$\mathscr{B} = \frac{\mu_{\alpha'}/\mu_\delta}{1 + f(\mu_{\alpha'}/\mu_\delta - 1)}. \tag{6}$$

$\mathscr{A}$ is the constant and has the same dimension as elastic modulus. The constant explains an inertial stress induced by the difference of creep strains between two matrixes. $\mathscr{B}$ explains the stress distribution coefficient. As discussed

in Section 3.2, correlations between creep strain rates in δ ferrite and α' martensite are summarized in Table 2. The following equations are formulated using the table. The inertial stress is not induced, because of $\varepsilon_{\alpha'} = \varepsilon_{\delta}$. $\sigma_{\alpha'}$ and σ_{δ} are consequently equal to the effective stresses, which can directly drive creep of matrixes. These stresses are expressed as follows:

$$\begin{cases} \sigma_{\alpha'} = \frac{1-f_{\delta}\mathscr{B}}{1-f_{\delta}}\sigma, \\ \sigma_{\delta} = \mathscr{B}\sigma. \end{cases} \tag{7}$$

Fig. 9 shows the results of characterizing the dual phase 9Cr-ODS steel as a composite. In Fig. 9(a), the effective stress decreases with increasing ratio of the shear modulus and/or volume fraction of the δ ferrite. In Fig. 9(b), the stress distribution constant increases with decreasing volume fraction of the δ ferrite and/or with increasing ratio of the shear modulus. These results quantitatively indicate the δ ferrite functions as a reinforcement. When considering these results, the exponential type equation can be modified and extended as follows:

$$\dot{\varepsilon}_i = \dot{\varepsilon}_{0,i} \exp\left(-\frac{Q_i - \sigma_i V_i}{RT}\right) \quad (i = \alpha', \delta). \tag{8}$$

Table 2
Correlations between creep strain rates

	Composite	α'	δ
Deformation	$\dot{\varepsilon} = \dot{\varepsilon}_{\alpha'} = \dot{\varepsilon}_{\delta}$	$\dot{\varepsilon}_{\alpha'} = \dot{\varepsilon}_{\mathrm{disl.},\alpha'} = \dot{\varepsilon}_{\mathrm{g.b.s.},\alpha'}$	$\dot{\varepsilon}_{\delta} = \dot{\varepsilon}_{\alpha'}$
Crack initiation and rupture	$\dot{\varepsilon}_{\alpha'} > \dot{\varepsilon}_{\delta}$	$\dot{\varepsilon}_{\mathrm{disl.},\alpha'} < \dot{\varepsilon}_{\mathrm{g.b.s.},\alpha'}$	$\dot{\varepsilon}_{\delta} \approx 0$

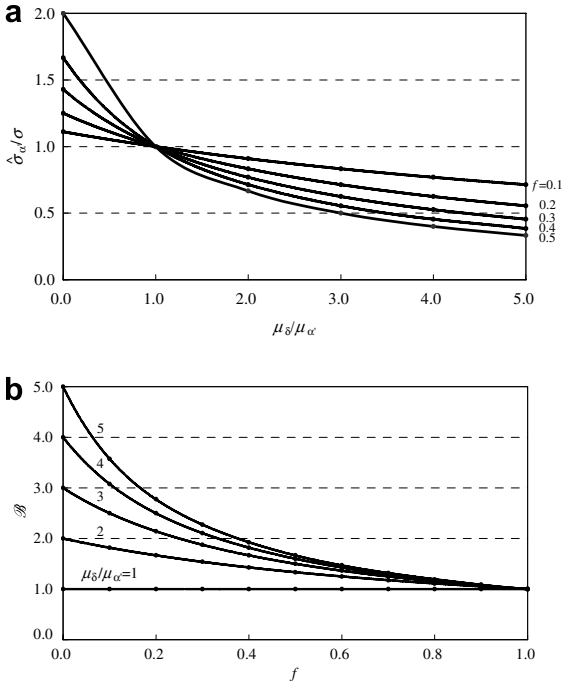

Fig. 9. Characterization of the dual phase 9Cr-ODS steel as a composite: (a) ratio of effective stress to applied stress and (b) stress distribution coefficient.

The following equation is the creep constitutive equations of the dual phase 9Cr-ODS steel.

$$\begin{cases} \dot{\varepsilon}_{\alpha'} = \dot{\varepsilon}_{0,\alpha'} \exp\left\{-\frac{Q_{\alpha'} - \left(\frac{1-f_{\delta}\mathscr{B}}{1-f_{\delta}}\right)\sigma V_{\alpha'}}{RT}\right\}, \\ \dot{\varepsilon}_{\delta} = \dot{\varepsilon}_{0,\delta} \exp\left(-\frac{Q_{\delta} - \mathscr{B}\sigma V_{\delta}}{RT}\right). \end{cases} \tag{9}$$

EOS in each phase can be calculated by the following equation:

$$\begin{cases} Q_i = Q_{\mathrm{d},i} + Q_{\mathrm{int},i}\left(1 - \frac{d\ln\mu_i}{d\ln T}\right), \\ \qquad\qquad (i = \alpha', \delta). \\ \frac{d_i}{p_i} = \frac{\mu_i b}{\pi(1-\nu)} \ln\left(\frac{d_i}{2r_{0,i}}\right)\frac{V_i}{Q_{\mathrm{int},i}}, \end{cases} \tag{10}$$

Eqs. (3) and (9) can be solved as identical equations, because of $\dot{\varepsilon} = \dot{\varepsilon}_{\alpha'} = \dot{\varepsilon}_{\delta}$. Using the calculated material constants, V_i and Q_i, and Eq. (10), EOS in the matrixes can be calculated. Fig. 10 shows the calculated EOS values. The EOS values in α' martensite and δ ferrite decrease with increasing strain and they approach steady values. These EOS value changes can interpret microstructural evolutions of the dual phase 9Cr-ODS steel. Based on the model of the exponential type equation [14], the decrease of EOS value means the increase of the obstacle dislocation density, indicating work hardening. The work hardening is observed in Fig. 5. The creep strain rate decrease with increasing time and strain. This behavior explains that the intragranular dislocation climb and glide mechanism became difficult to function and to relax the strain induced by the grain boundary sliding, as discussed in the Section 3.2. The steady EOS values in α' martensite and δ ferrite are comparable to the experimental oxide particle spacing values, which are about 45 nm in α' martensite and about 30 nm in δ ferrite observed by TEM [1]. Eq. (9) is consequently available as the creep constitutive equation of the dual phase 9Cr-ODS steel.

These calculated EOS steady values were slightly larger than the observed values. The difference between the calculated EOS steady values and the observed values results from the insufficient sampling rate of creep rupture tests. Approximative usage of the shear modulus and its

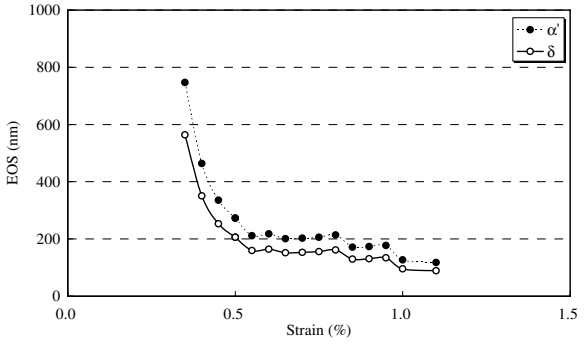

Fig. 10. Calculated obstacle spacing at 973 K using the extended exponential type equation.

temperature dependence also affected the differences. The creep rupture test with increased sampling rate and appropriate usages of the shear modulus and its time dependence can reduce the differences between calculated and observed values. Although further microstructural observations and investigations into details are required to calculate the creep strain rate using the creep constitutive equation, the correlation between microstructures and creep properties are quantitatively shown in this study.

4. Summary

A novel creep constitutive equation was formulated based on detailed microstructural observations, to develop reliable life prediction methods. The 9Cr-ODS steel displaying an excellent creep property was a dual phase steel. The ODS steel is consist of α' martensite and δ ferrite, and it was characterized as a composite. Microstructural observations revealed the creep mechanism that the grain boundary sliding mechanism in α' martensite cooperates with the intragranular dislocation climb and glide mechanism in α' martensite. The creep strain rate can be accordingly represented by the rate of intragranular dislocation climb and glide creep mechanism, and the exponential type equation is consequently applied. The equation based on a physical model was modified and extended by the law of mixture, to formulate the creep constitutive equation of the dual phase 9Cr-ODS steel.

The alternative creep constitutive equation can quantitatively interpret the creep mechanism of the dual phase 9Cr-ODS steel and it can calculate oxide particle spacing as EOS. In future works, the creep strain will be calculated using the equation, based on further microstructural observations and investigations into details.

References

[1] S. Ukai, M. Fujiwara, J. Nucl. Sci. Technol. 39 (2002) 778.
[2] S. Ukai, T. Kaito, S. Ohtsuka, T. Narita, M. Fujiwara, T. Kobayashi, ISIJ Int. 43 (2003) 2038.
[3] S. Ohtsuka, S. Ukai, M. Fujiwara, T. Kaito, T. Narita, J. Nucl. Mater. 329-333 (2004) 372.
[4] S. Ohtsuka, S. Ukai, M. Fujiwara, T. Kaito, T. Narita, Mater. Trans. 46 (2005) 487.
[5] S. Ohtsuka, S. Ukai, M. Fujiwara, J. Nucl. Mater. 351 (2006) 241.
[6] R.L. Klueh, J.P. Shingledecker, R.W. Swindeman, D.T. Hoelzer, J. Nucl. Mater. 341 (2005) 103.
[7] M.J. Alinger, G.R. Odette, D.T. Hoelzer, J. Nucl. Mater. 329-333 (2004) 382.
[8] H. Kishimoto, M.J. Alinger, G.R. Odette, T. Yamamoto, J. Nucl. Mater. 329–333 (2004) 369.
[9] G. Yu, N. Nita, N. Baluc, Fusion Eng. Des. 75–79 (2005) 1037-1.
[10] I. Tamura, T. Tomoda, Y. Yamada, S. Knatani, M. Ozawa, A. Akao, Tetsu to Hagane 3 (1973) 96.
[11] H. Sakasegawa, S. Ohtsuka, S. Ukai, H. Tanigawa, M. Fujiwara, H. Ogiwara, A. Kohyama, Fusion Eng. Des. 81 (2006) 1013.
[12] H. Sakasegawa, S. Ohtsuka, S. Ukai, H. Tanigawa, M. Fujiwara, H. Ogiwara, A. Kohyama, J. Nucl. Mater., in press, doi:10.1016/j.jnucmat.2007.03.148.
[13] M. Tamura, H. Esaka, K. Shinozuka, ISIJ Int. 39 (1999) 380.
[14] M. Tamura, H. Esaka, K. Shinozuka, Mater. Trans. 41 (2000) 272.
[15] M. Tamura, H. Esaka, K. Shinozuka, Mater. Trans. 44 (2003) 118.
[16] M. Tamura, H. Sakasegawa, A. Kohyama, K. Shinozuka, H. Esaka, TMS Letters 1 (5) (2004) 109.
[17] K. Wakashima, T. Moriyama, T. Mori, Acta Mater. 48 (2000) 891.
[18] K. Wakashima, Materia 40 (2) (2001) 122.